The Astrophysical Journal, 853:30 (7pp), 2018 January 20 https://doi.org/10.3847/1538-4357/aaa023

Stellar Parameters for Trappist-1

Valérie Van Grootel[1], Catarina S. Fernandes[1], Michael Gillon[1], Emmanuel Jehin[1], Jean Manfroid[1], Richard Scuflaire[1], Adam J. Burgasser[2,3], Khalid Barkaoui[1,4], Zouhair Benkhaldoun[4], Artem Burdanov[1], Laetitia Delrez[5], Brice-Olivier Demory[6], Julien de Wit[7], Didier Queloz[5], and Amaury H. M. J. Triaud[8]
[1] Space Sciences, Technologies and Astrophysics Research (STAR) Institute, Université de Liège, 19C Allée du 6 Août, B-4000 Liège, Belgium
valerie.vangrootel@uliege.be
[2] Center for Astrophysics and Space Science, University of California San Diego, La Jolla, CA 92093, USA
[3] Fulbright Scholar, University of Exeter, College of Engineering, Mathematics and Physical Sciences, Exeter EX4 4QL, UK
[4] Laboratoire LPHEA, Oukaimeden Observatory, Cadi Ayyad University/FSSM, BP 2390, Marrakesh, Morocco
[5] Cavendish Laboratory, J.J. Thomson Avenue, Cambridge CB3 0HE, UK
[6] University of Bern, Center for Space and Habitability, Gesellschaftsstrasse 6, CH-3012, Bern, Switzerland
[7] Department of Earth, Atmospheric and Planetary Sciences, Massachusetts Institute of Technology, 77 Massachusetts Avenue, Cambridge MA 02139, USA
[8] School of Physics & Astronomy, University of Birmingham, Edgbaston, Birmingham B15 2TT, UK
Received 2017 October 24; revised 2017 December 2; accepted 2017 December 5; published 2018 January 19

Abstract

TRAPPIST-1 is an ultracool dwarf star transited by seven Earth-sized planets, for which thorough characterization of atmospheric properties, surface conditions encompassing habitability, and internal compositions is possible with current and next-generation telescopes. Accurate modeling of the star is essential to achieve this goal. We aim to obtain updated stellar parameters for TRAPPIST-1 based on new measurements and evolutionary models, compared to those used in discovery studies. We present a new measurement for the parallax of TRAPPIST-1, 82.4 ± 0.8 mas, based on 188 epochs of observations with the TRAPPIST and Liverpool Telescopes from 2013 to 2016. This revised parallax yields an updated luminosity of $L_* = (5.22 \pm 0.19) \times 10^{-4}\, L_\odot$, which is very close to the previous estimate but almost two times more precise. We next present an updated estimate for TRAPPIST-1 stellar mass, based on two approaches: mass from stellar evolution modeling, and empirical mass derived from dynamical masses of equivalently classified ultracool dwarfs in astrometric binaries. We combine them using a Monte-Carlo approach to derive a semi-empirical estimate for the mass of TRAPPIST-1. We also derive estimate for the radius by combining this mass with stellar density inferred from transits, as well as an estimate for the effective temperature from our revised luminosity and radius. Our final results are $M_* = 0.089 \pm 0.006\, M_\odot$, $R_* = 0.121 \pm 0.003\, R_\odot$, and $T_{\rm eff} = 2516 \pm 41$ K. Considering the degree to which the TRAPPIST-1 system will be scrutinized in coming years, these revised and more precise stellar parameters should be considered when assessing the properties of TRAPPIST-1 planets.

Key words: stars: individual (TRAPPIST-1) – stars: late-type – stars: low-mass

1. Introduction

TRAPPIST-1 (2MASS J23062928-0502285) is an ultracool M8 dwarf star located 12 pc from the Sun (Gizis et al. 2000; Costa et al. 2006). It hosts seven Earth-sized planets, of which three orbit in the habitable zone (Gillon et al. 2017). It is the first planetary system found to transit such an extremely low-mass, Jupiter-sized star. This favorable planet-to-star ratio opens up the possibility of thoroughly characterizing the exoplanets, including probing their atmospheric properties, with current and next-generation telescopes (Barstow & Irwin 2016; de Wit et al. 2016; Bourrier et al. 2017). TRAPPIST-1 is a unique system for testing planet formation and evolution theories, and for assessing the prospects for habitability among Earth-sized exoplanets orbiting cool M dwarfs, the most numerous stars in the Galaxy (Bochanski et al. 2010). Finally, TRAPPIST-1 is a golden target for comparative exoplanetology, by contrasting the atmospheric properties, surface conditions, and internal compositions of similar exoplanets orbiting the same star. Determining exoplanetary properties relies on a detailed knowledge of the host star, notably as observations mostly constrain them relatively to those of the host. In particular, the irradiation of the planets scales as L_*/a^2, where L_* is the stellar luminosity and a is the semimajor axis of the orbit, which depends on the stellar mass through *Kepler*'s third law (Seager & Deming 2010). The transit depth measures the planet-to-star radius ratio, and hence inference of the planet radius requires knowledge of the stellar radius (Winn 2010). The transformation of the planetary mass ratios determined by transit timings variations (TTVs) into the planet physical parameters rely on the stellar mass (Agol et al. 2005). A crucial element in assessing the ability of a planet to retain an atmosphere, therefore its long-term habitability, is the time its host star takes to contract onto the main sequence (e.g., Luger & Barnes 2015). This time is acutely sensitive to stellar parameters for very low-mass stars, and contraction time rapidly increases to several gigayears below $\sim$0.10 $M_\odot$ (e.g., Chabrier & Baraffe 1997; Chabrier et al. 2000; Baraffe et al. 2015, hereafter BHAC15; see also our Figure 3).

TRAPPIST-1 is an M8.0 $\pm$ 0.5 star (Gillon et al. 2016; see also, e.g., Gizis et al. 2000; Costa et al. 2006; Burgasser et al. 2015; Burgasser & Mamajek 2017). Its luminosity ($\log L_*/L_\odot = -3.28 \pm 0.03$ or $L_* = (5.25^{+0.38}_{-0.35}) \times 10^{-4}\, L_\odot$) has been determined by Filippazzo et al. (2015) from a nearly complete spectral energy distribution and the parallax measurement of Costa et al. (2006). The iron abundance of TRAPPIST-1, [Fe/H] $= 0.04 \pm 0.08$ (Gillon et al. 2016), has been estimated from the calibration of Mann et al. (2014). The prior probability distribution functions (PDFs) that were used by Gillon et al. (2016, 2017) for stellar mass, radius, and effective temperature are $M_* = 0.082 \pm 0.011\, M_\odot$, $R_* = 0.114 \pm 0.006\, R_\odot$, and

$T_{\rm eff} = 2555 \pm 85$ K, respectively. The mass and radius estimates come from evolutionary models, combining estimates from Filippazzo et al. (2015) mainly based on Chabrier et al. (2000) models, and our own estimates based on more recent BHAC15 models (details about this can be found in the "Methods" section of the supplementary information of Gillon et al. 2016). The estimate for effective temperature was obtained by combining the model radius and the luminosity from Filippazzo et al. (2015). Filippazzo et al. (2015) constrained the age to be higher than 500 Myr in the absence of any sign of youth, but an age of about 500 Myr is actually inferred from Chabrier et al. (2000) or BHAC15 evolutionary models for a $\sim$0.082 $M_{\odot}$ star at the luminosity of Filipazzo (see also our Section 4 and Figure 3).

However, TRAPPIST-1 is most likely not a young star, as recently argued by Burgasser & Mamajek (2017), who examined all available age indicators for TRAPPIST-1. Combining age probability distribution functions from metallicity and kinematics, and lower limits from the absence of lithium absorption and measured rotation period, Burgasser & Mamajek (2017) inferred an age of 7.6 ± 2.2 Gyr. The authors also proposed, based on this old age estimate and the observed luminosity, revising the stellar radius upward to $R_{*} = 0.121 \pm 0.003\ R_{\odot}$. They obtained this radius by artificially "inflating" the radii obtained by the evolutionary models of Burrows et al. (1997, 2001) and BHAC15 to account for the stellar density inferred from transits. It is indeed well known that current stellar models tend in many cases to underestimate stellar radii for low-mass stars (e.g., Reid & Hawley 2005; Spada et al. 2013; Feiden & Chaboyer 2014b; MacDonald & Mullan 2014, and references therein). Burgasser & Mamajek (2017) proposed that metallicity and/or magnetic activity effects are possible culprits for this radius inflation of TRAPPIST-1. However, without published evolutionary models that account for these effects, the authors were unable to validate this hypothesis.

We present in this paper updated stellar parameters for TRAPPIST-1. We present a new parallax estimate in Section 2, allowing us to derive a more precise stellar luminosity. We next derive an updated stellar mass estimate for TRAPPIST-1, based on two approaches: an empirical mass derived from dynamical masses of equivalently classified ultracool dwarfs in astrometric binaries (Section 3), and a stellar mass from evolution modeling that is able to take into account metallicity and magnetic activity effects (Section 4). We combine the information from evolutionary models and dynamical masses in Section 5 to obtain final stellar parameters for TRAPPIST-1. We conclude in Section 6.

2. New Parallax and Luminosity Estimates

In order to improve the distance and then luminosity measurements of TRAPPIST-1, we analyzed all of the optical data collected during the monitoring of TRAPPIST-1 in order to obtain its parallax as precisely as possible. Most data are from the UCDTS survey carried out with TRAPPIST-South (TS) located in the La Silla Observatory in Chile (Jehin et al. 2011; Gillon et al. 2011). This data set consists of 33,118 images distributed among a total of 114 epochs regularly collected from May to December in 2013, 2015, and 2016. They have been complemented with 10,969 images obtained in 2016 in 61 epochs with TRAPPIST-North (TN), located at the Oukaimeden Observatory in Morocco, and 3,302 images in 13 epochs in 2015 and 2016 obtained with the Liverpool Telescope (LT; Steele et al. 2004) in La Palma. The TS and

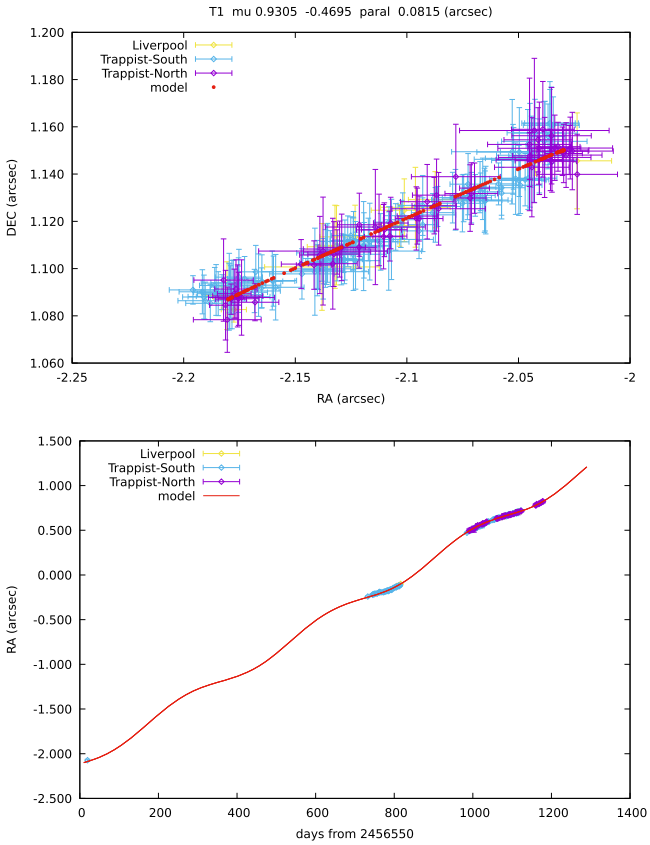

Figure 1. Top: R.A.–decl. parallactic displacement after subtraction of the proper motion (arbitrary origin). Bottom: R.A. motion of TRAPPIST-1 as a function of the date (in days).

TN images have been taken with an I + z filter and 2048 × 2048 pixel CCD cameras of 15 and 13μm, providing plate scales of 0.″655 and 0.″60 per pixel and covering fields of view of 22′ and 20′, respectively. The LT data have been taken using the IO:O camera and a Sloan z' filter, and have a plate scale of 0.″30 per 2 × 2 binned pixel and a 10′ field of view. Each data set has been reduced separately using standard bias, dark, and flat field correction techniques. Each epoch is a clear night for which there are at least 20 images spanning an hour angle of maximum 2.5 hr and for which we have obtained an astrometric solution with a rms <0.″08, after keeping always the same best 65 stars having coordinates in the 2MASS catalog. The model to fit the data is simply a constant proper motion and the periodic oscillation of the parallax. The best fit of all the data together gives a relative parallax of 0.″0815 and R.A. and decl. proper motions of 0.″9305 and −0.″4695, respectively (Figures 1 and 2). The fit to the individual data sets gives for the parallax and the proper motions (0.″081; 0.″931; −0.″473) for TS, (0.″082; 0.″931; −0.″469) for TN, and (0.″083; 0.″934; −0.″469) for LT, respectively. This is in good agreement with the fit to the whole data set and allows us to also provide error bars from a weighted mean of the three data sets, giving for TRAPPIST-1 RAC and decl. proper motions of $0.''9305 \pm 0.''0005$, and $-0.''4695 \pm 0.''0005$, respectively, and a relative parallax of $0.''0815 \pm 0.''0006$.

For the offset correction of the background reference stars to apply in order to obtain the absolute parallax, we used the mean value of Costa et al. (2006; 0.68 mas) and Boss et al. (2017; 1.08 mas), or 0.88 ± 0.20 mas. They both have fields of view

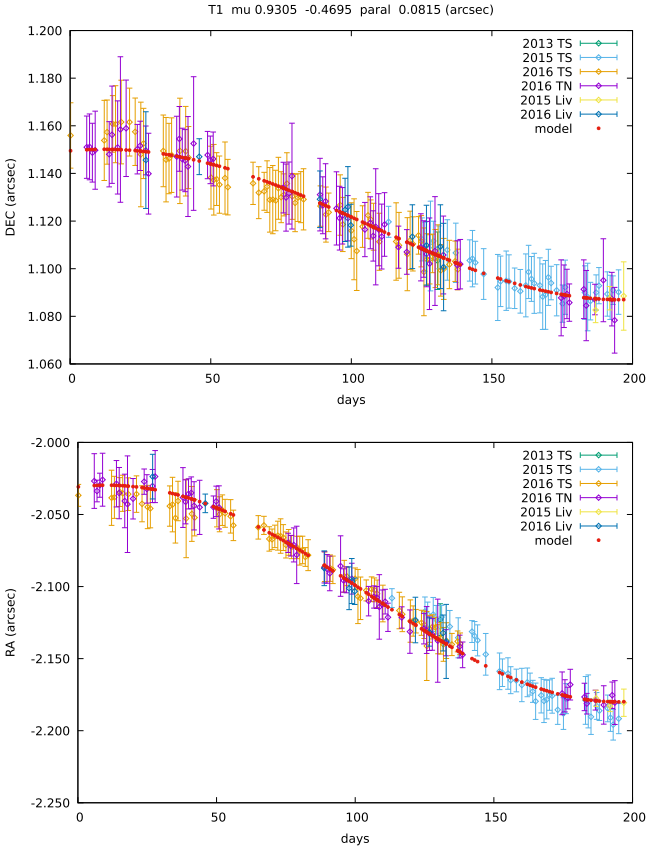

Figure 2. Top: decl. parallactic displacement as a function of the date, modulo 1 year (arbitrary origin). Bottom: same, but for R.A.

similar to ours, use near-IR (NIR) filters like us, and have used stars in common to ours.

We then get a final value of the absolute parallax of 82.4 ± 0.8 mas (distance $d = 12.14 \pm 0.12$ pc). This measurement is in very good agreement with the parallax of 82.58 ± 2.7 mas provided by Costa et al. (2006), computed from eight epochs and spanning three years. Our value is in disagreement with the more recent value of 79.59 ± 0.78 mas published by Boss et al. (2017), based mostly on the data from Weinberger et al. (2016) and using 15 epochs from 2011 to 2016. In the latter study they noticed that their parallaxes are about 2.5 mas smaller than those of stars in common with several other studies, which is about the difference we also find for TRAPPIST-1. An exquisite and definitive parallax value for TRAPPIST-1 should be obtained in coming years from *Gaia* data, with expected error as low as 0.05 mas, 10 times better at least than our value.

Using our final value of the absolute parallax and the spectral energy distribution of Filippazzo et al. (2015), we revised the luminosity of TRAPPIST-1 to $L_* = (5.22 \pm 0.19) \times 10^{-4}\, L_\odot$, almost two times better than the previous uncertainties from Filippazzo et al. (2015).

3. Empirical Mass from Astrometric Binaries

We made a first determination of the mass of TRAPPIST-1 using the dynamical masses inferred for a sample of ultracool dwarfs in astrometric binaries (Dupuy & Liu 2017, hereafter DL17). We selected 20 objects from the sample of DL17 that have a spectral type between M6 and L1.5, close to the one of TRAPPIST-1. We then used the NIR colors, luminosity, and mass of these 20 objects, and their associated errors from DL17, to estimate the mass of TRAPPIST-1 through the following Monte-Carlo approach. We performed an analysis composed of 100,000 independent steps. At each step, we drew a value for the luminosity and $J-K$ color index of TRAPPIST-1, from the normal distributions centered on 5.22×10^{-4} and 1.058 with standard deviations of 1.9×10^{-5} and 0.001, respectively. At each step, we also did the same for the 20 selected ultracool objects, drawing from the normal distributions corresponding to the values and errors from DL17. For each object i, the agreement between its luminosity and its $J-K$ index and those of TRAPPIST-1 was estimated—for both parameters—with the following formula:

$$\delta x = \frac{|x_{T1} - x_i|}{\sqrt{(\sigma^2_{x_{T1}} + \sigma^2_{x_i})}} \quad (1)$$

where x is L_* or $J-K$ index, and σ_x is its associated error, for TRAPPIST-1 (T1) or the object i. If δx was larger than 1 for one of the two parameters, the object was discarded. For the remaining objects, a value of the mass was then drawn from the normal distribution corresponding to their mass measurement and error from DL17, and stored. At the end of the 100,000 steps, we obtained a resulting mass PDF with mean and standard deviation of $M_* = 0.090 \pm 0.012\, M_\odot$. The exact same results were obtained using $H-K$ or $J-H$ color indexes.

4. Stellar Mass from Evolution Modeling

4.1. Evolutionary Models for Very Low-mass Stars

We adapted our stellar evolution code CLES (Code Liégeois d'Evolution Stellaire) to compute structures of very low-mass stars (VLMS). We refer to Scuflaire et al. (2008) for the main constitutive physics and numerical features, but here are the details specific to VLMS. Two aspects are of particular relevance for computing structures of VLMS (Chabrier & Baraffe 1997): the surface boundary conditions, which must be extracted from detailed model atmospheres, and the equation of state (EOS), which must cover the dense and cool regime of VLMS. We extracted boundary conditions from the publicly available BT-Settl model atmospheres (Allard et al. 2012a, 2012b; Rajpurohit et al. 2013) computed with the solar abundances of Asplund et al. (2009). Several compositions are publicly available, from $Z_{\rm ini} \sim 0.004$ to $\sim$0.04. We also used the solar abundances of Asplund et al. (2009) to compute the interior structure. The transition interior/atmosphere is performed at an optical depth $\tau = 100$, similar to the stellar evolution models of BHAC15 that are the commonly used reference for VLMS. For the EOS, we considered H, He, C, and O. We directly adapted tables built for white dwarfs and subdwarf B stars kindly made available to us by G. Fontaine. These tables cover a large domain of the temperature-density plane including VLMS (details are given in Van Grootel et al. 2013). In a nutshell, in the partial ionization region where nonideal and degeneracy effects are important, we used the EOS of Saumon et al. (1995) for H and He, an improved version of the EOS of Fontaine et al. (1977) for C, and similar developments for the EOS of O. Interpolation in composition is handled following the additive volume prescription of Fontaine et al. (1977). We used opacities from the OPAL project (Iglesias & Rogers 1996), combined for low temperatures to

opacities from Ferguson et al. (2005). The effects of thermal conductivity have been taken into account according to the computations of Potekhin et al. (1999) and Cassisi et al. (2007). Nuclear reaction rates, for De and Li burning, as well as for the pp chain, come from the NACRE II compilation (Xu et al. 2013). Convection is treated using the mixing length theory (MLT). For ultracool stars, we set $\alpha_{\rm MLT}$ (the ratio between the mixing length and the pressure scale height) to 2.0, according to recent 3D radiative hydrodynamic (RHD) simulations, showing that the calibrated $\alpha_{\rm MLT}$ increases to this value for the coolest and densest stars (Magic et al. 2015). Our solar calibration (evolutionary track giving the Sun at the right age, luminosity, and effective temperature, here without diffusion) gives $\alpha_{\rm MLT} = 1.8$, $X_{\rm ini} = 0.728$, and $Z_{\rm ini} = 0.013$. Our initial helium abundance is therefore close to the initial helium abundance of Bt-Settl model atmospheres, which is $Y_{\rm ini} = 0.249$ (with Asplund et al. 2009 solar mixture). BHAC15, however, showed that the exact consistency of $Y_{\rm ini}$ between interior structure and model atmosphere is not a source of tension, especially for VLMS (see their Section 4.2).

A comparison between CLES and BHAC15 models is provided on Figure 3 that shows evolutionary tracks for 0.08, 0.09, and 0.10 $M_{\odot}$ star with, as far as possible, identical constitutive physics (Grevesse & Noels 1993 for the interior/ Asplund et al. 2009 supplemented by Caffau et al. 2011 for some elements for the boundary conditions; EOS for H and He only; Chabrier & Baraffe 1997; BHAC15). BHAC15 and CLES stellar tracks are very close. For a given mass, CLES models tend to provide very similar luminosity with a slightly larger (by $\sim$+3%) stellar radius, and therefore a lower stellar density, and slightly lower effective temperature (by ~-30 K) estimates compared to BHAC15 models. Our CLES models, therefore, have similar strengths and weaknesses than BHAC15 models: they tend to provide accurate estimates for the mass and the luminosity, while they tend to underestimate the radius and overestimate the effective temperature (e.g., Reid & Hawley 2005; Spada et al. 2013; Torres 2013; Dupuy & Liu 2017, and references therein). This is not a systematic trend, however, as some stars are consistent with theoretical estimates (Spada et al. 2013; Kervella et al. 2016; von Boetticher et al. 2017).

4.2. Modeling TRAPPIST-1

We performed stellar evolution modeling for TRAPPIST-1 using our in-house Levenberg–Marquardt optimization algorithm (Press et al. 1992). Three independent measurements were used to constrain stellar models: luminosity (see Section 2), age (Burgasser & Mamajek 2017), and density inferred from transits. We took the most recent value inferred for the most complete observational data set (Delrez et al. 2018) $\rho_{*} = 51.1^{+1.2}_{-2.4}\,\rho_{\odot}$. Assuming all elements scale like in the Sun, the iron abundance of TRAPPIST-1, [Fe/H] = 0.04 ± 0.08, corresponds to a Z/X ratio of the models of 0.020 ± 0.004. In all stellar evolution modeling, the reference values are given for $Y_{\rm ini} = 0.26$, the initial helium abundance of the Sun according to our solar calibration.

4.2.1. First Case: Luminosity and Density as Constraints, no Age Indication

First, we checked with our CLES models the stellar estimates used as priors in transit analyses (see the Introduction

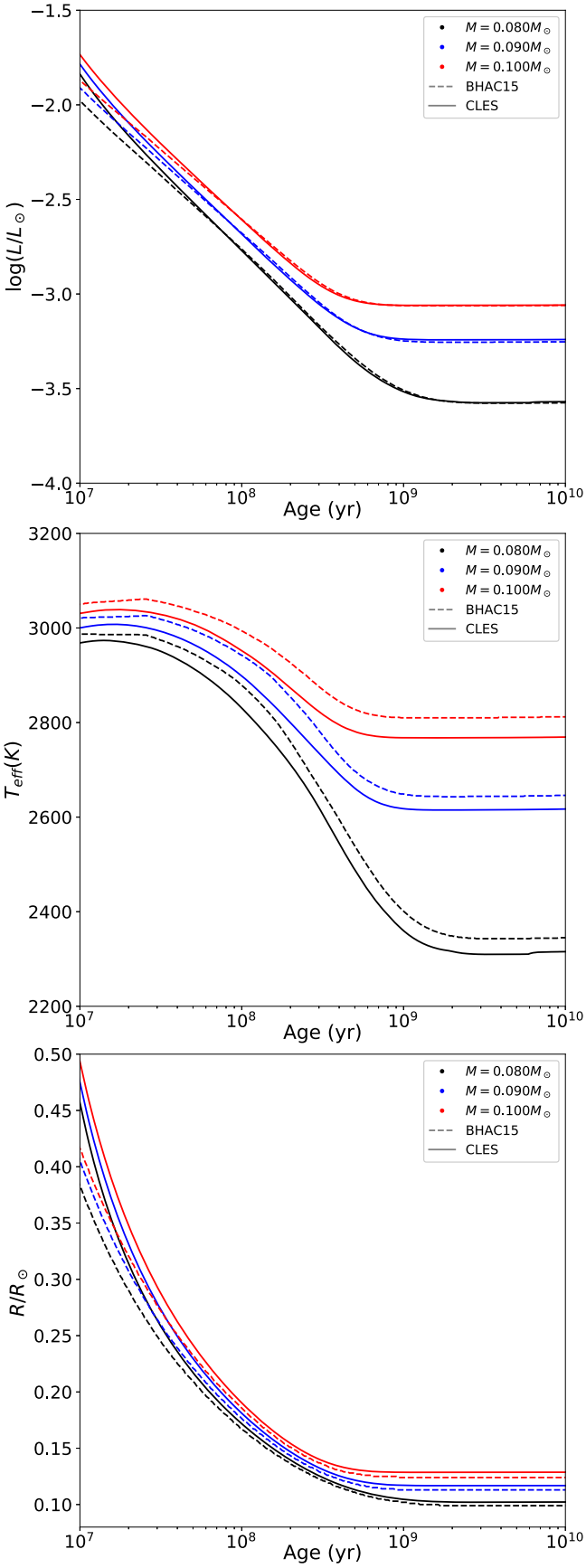

Figure 3. Comparison between CLES and BHAC models for very similar input physics, for luminosity (top panel), effective temperature (middle panel), and radius (bottom panel), for 0.08, 0.09 and 0.10 $M_{\odot}$.

and Gillon et al. 2016, 2017). No indication on the age of TRAPPIST-1 was available at that time. Using stellar density and luminosity as constraints, we obtained a stellar mass $M_* = 0.081 \pm 0.003\,M_\odot$ and age $= 450 \pm 55$ Myr, which corresponds to model radius $R_* = 0.117 \pm 0.002\,R_\odot$ and model effective temperature $T_{\rm eff} = 2555 \pm 25$ K. These errors come from errors L_*, ρ_* and Z/X, based on error propagation with full evolutionary tracks. More precisely, we computed various evolutionary tracks by varying observational constraints (L_*, ρ_* and Z/X) within their given 1-σ range and computed the respective 1-σ confidence interval for M_*, R_*, $T_{\rm eff}$, and age.

The parameters we derived with CLES models are in complete agreement with those used for transit analyses (see the Introduction and Gillon et al. 2016, 2017). As previously noticed, this corresponds to a young age for TRAPPIST-1, which is now disputed (Burgasser & Mamajek 2017). The priors on stellar parameters must then be revised.

4.2.2. Second Case: Luminosity and Age as Constraints

Second, we performed stellar evolution modeling using luminosity and age as constraints only, given the discrepancies of the models toward radius and effective temperature. It can be seen directly in Figure 4 (top panel) that a stellar mass of $\sim$0.09 $M_\odot$ is needed to account for the old age and luminosity of TRAPPIST-1. More quantitatively, we found a stellar mass of $M_* = 0.089 \pm 0.003\,M_\odot$ for an age between 2–15 Gyr (evolution models are not able to provide a precise stellar age, as the star evolves extremely slowly). This error was computed as in Section 4.2.1, and it also took into account the unknown initial helium abundance, which varied from $Y = 0.25$ (primordial value) to $Y = 0.30$, a reasonable assumption for a field star like TRAPPIST-1 (see, for instance, Metcalfe et al. 2014 for the initial helium abundance of 42 *Kepler* stars inferred from asteroseismology). These errors have been quadratically added to the previous ones. The corresponding model radius is $R_* = 0.114 \pm 0.002\,R_\odot$ and effective temperature is $T_{\rm eff} = 2595 \pm 30$ K. Let us note here that systematic errors of stellar models are notoriously difficult to estimate. We varied the depth of the transition between interior and atmosphere (from the reference at $\tau = 100$ up to the photosphere), as well as the $\alpha_{\rm MLT}$ parameter of convection (from solar to the reference value) and the opacities (using Opacity Project (OP) table rather than OPAL; Badnell et al. 2005). No significant difference on the results have been found. Other constitutive physics cannot be easily varied (in particular, no other EOS is currently available for the high-density, low-temperature domain encompassed by compact objects with masses below 0.1 $M_\odot$).

4.2.3. Third Case: Luminosity, Density, and Age as Constraints

Finally, we used luminosity, age, and density as constraints for stellar evolution modeling. At solar metallicity, no reasonable fit was found. Indeed, it can be seen directly in Figure 4 that the stellar density at $\sim 0.09 M_\odot$ would be much higher than the value measured from transits, due to a too-low stellar radius (Figure 5). As already noted, the CLES models do not perform better than the BHAC15 models with regard to the radius (and then stellar density) discrepancies. The usual suspects for this radius anomaly are the presence of strong magnetic field and/or magnetic activity such as spots, causing the stars to inflate by inhibiting convective energy transport (Mullan & MacDonald 2001; Chabrier et al. 2007), or increased metallicity compare to solar, causing the star to inflate due to increased stellar material opacity (Feiden & Chaboyer 2014b).

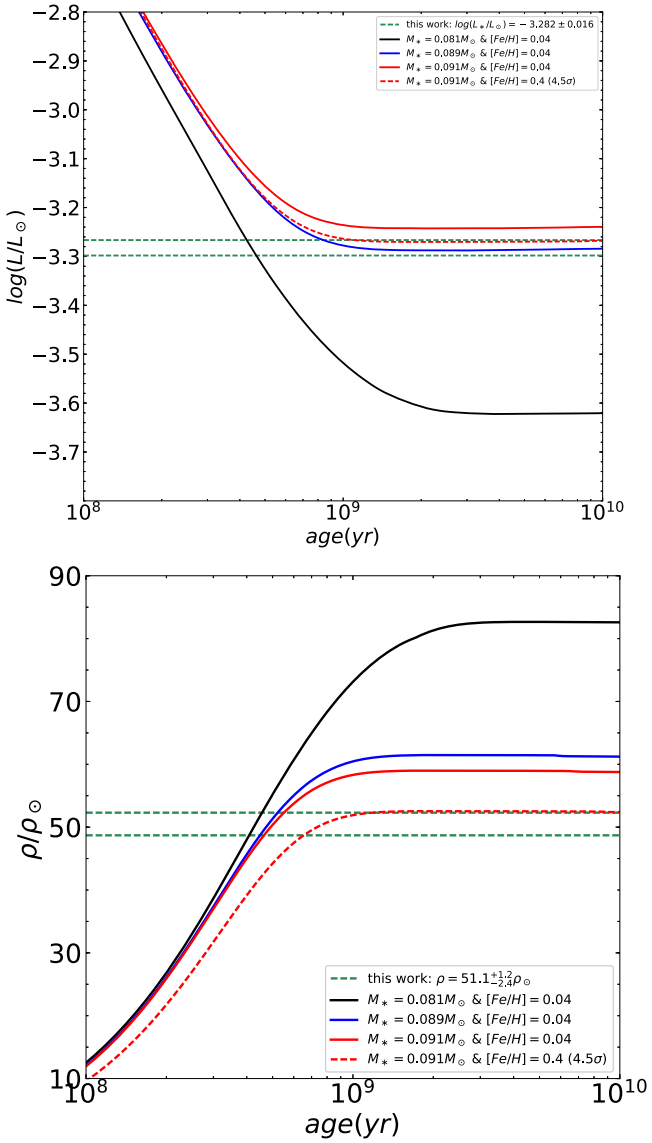

Figure 4. Stellar luminosity (top panel) and density (bottom panel) for evolution models for various masses and metallicities, compared to luminosity and density estimates for TRAPPIST-1 (dashed horizontal lines).

We empirically found that by doubling the Z/X ratio (corresponding to [Fe/H] = 0.40, a $+4.5\sigma$ error on the available estimate), we were able to reconcile stellar density and luminosity with the old age of Burgasser & Mamajek (2017). By performing a new Levenberg–Marquardt optimization, we found a stellar mass of $M_* = 0.091 \pm 0.005\,M_\odot$ for an age between 2–15 Gyr. The corresponding model radius is $R_* = 0.120 \pm 0.002\,R_\odot$ and effective temperature is $T_{\rm eff} = 2530 \pm 35$ K. The quoted errors are computed as previously.

Very similar results with a good fit to luminosity and density at old age were obtained by greatly reducing convection efficiency (down to $\alpha_{\rm MLT} \sim 0.05$). The two usual suspects for radius inflation, metallicity and magnetic activity effects, are therefore potentially accountable for the stellar density of

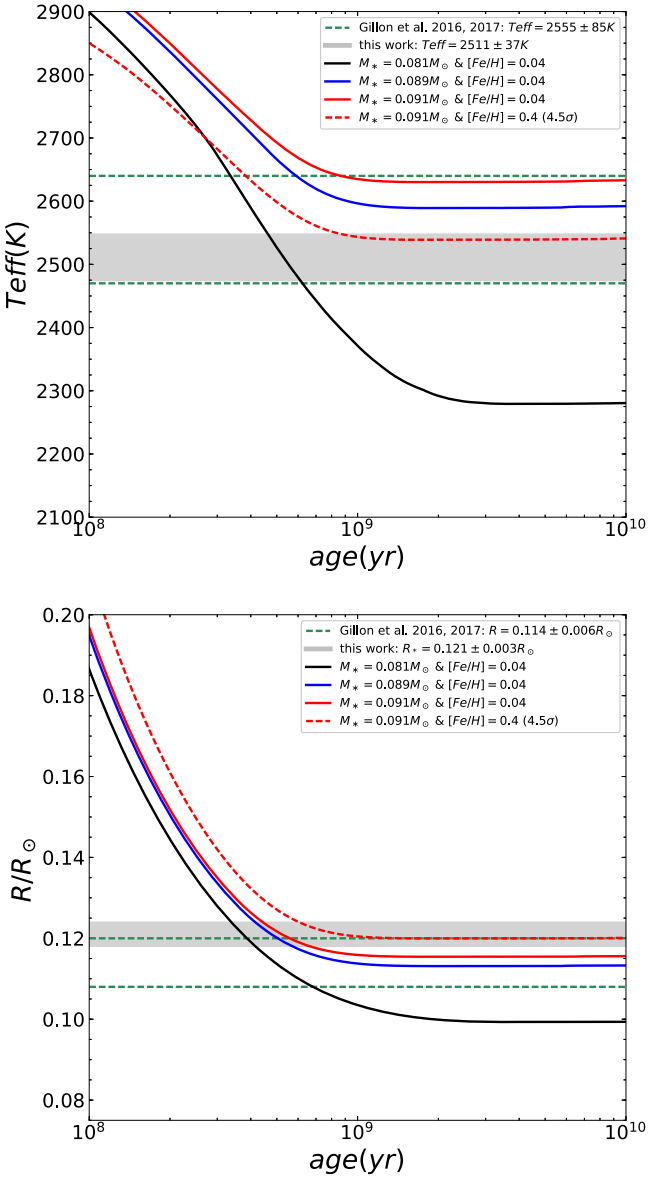

Figure 5. Effective temperature (top panel) and stellar radius (bottom panel) for evolution models for various masses and metallicities. Horizontal dashed lines shows the previous prior $T_{\rm eff}$ and R_* PDFs used for deriving planetary parameters (Gillon et al. 2017), and gray areas represent updated estimates from this work.

TRAPPIST-1. TRAPPIST-1 lies at the transition between thin and thick disk (Burgasser et al. 2015; Burgasser & Mamajek 2017). It is possible that the [Fe/H] measurement obtained by NIR spectroscopy (Gillon et al. 2016) is biased toward lower values by C and O abundances, which affect the pseudo-continuum level (Veyette et al. 2016). Investigations of high-resolution spectra to identify α-elements abundances and determine TRAPPIST-1 metallicity are yet to be made. Although rare, supermetallic stars such as Alpha Cen exist in the solar neighborhood (Miglio & Montalbán 2005; Porto de Mello et al. 2008). On the other hand, a convection parameter $\alpha_{\rm MLT} \sim 0.05$ is a huge reduction of the convection efficiency. Feiden & Chaboyer (2014a) demonstrated that magnetic stellar models are indeed unable to significantly inflate fully convective stars, unless extremely strong interior magnetic fields are present, and/or there is high coverage clustered at poles' star spots. TRAPPIST-1 is a low-activity M8 star

Table 1
Updated Stellar Parameters of TRAPPIST-1

Quantity	Value
$L_*/L_\odot$	0.000522 ± 0.000019
$M_*/M_\odot$	0.089 ± 0.006
$R_*/R_\odot$ [a]	0.121 ± 0.003
$T_{\rm eff}$(K) [b]	2516 ± 41

Notes.
[a] From M_* and ρ_*.
[b] From L_* and R_*.

(Luger et al. 2017) with a moderate surface magnetic field of 600^{+200}_{-400} G (Reiners & Basri 2010), for which an interior magnetic field of several MG (necessary to significantly inflate the star) is difficult to imagine. Brightness inhomogeneities are indeed present on TRAPPIST-1 (Luger et al. 2017), but a full analysis to determine their coverage and repartition over the star to confirm or refute this hypothesis has yet to be done.

Alternatively, such enhanced metallicity or convection reduction may actually correspond to missing/perfectible constitutive physics in stellar models, related to opacities, model atmospheres, or EOS. We will investigate these possibilities in forthcoming papers.

5. Final Stellar Parameters for TRAPPIST-1

Finally, we combined the information from stellar evolution models and ultracool dwarf binaries to obtain final stellar parameters for TRAPPIST-1. Given the discrepancies of stellar models toward radius and effective temperature, we relied on the stellar mass obtained by using only luminosity and age as constraints (Section 4.2.2). We carried out the same Monte-Carlo analysis described in Section 3, except for the following. At each step, for each tested ultracool object from DL17 the value drawn for its mass was compared to a value drawn from the distribution $N(0.089, 0.003^2)$, again using Equation (1) to discard values disagreeing with each other at more than 1-σ. We obtained $M_* = 0.089 \pm 0.006\,M_\odot$.

At each step of the analysis we also drew values for the density and luminosity of TRAPPIST-1 based on the measurements $\rho_* = 51.1^{+1.2}_{-2.4}\,\rho_\odot$ (Delrez et al. 2018) and $L_* = (5.22 \pm 0.19) \times 10^{-4}\,L_\odot$ (Section 2), enabling a computation of a value for the stellar radius (from ρ_* and M_*) and for the effective temperature (from $L_* = 4\pi R_*^2 \sigma T_{\rm eff}^4$). The means and standard deviations of the distributions resulting from the 100,000 steps are $R_* = 0.121 \pm 0.003\,R_\odot$ and $T_{\rm eff} = 2516 \pm 41$ K. We adopt these values and errors as our updated stellar parameters for TRAPPIST-1 simply suppress this. These values are summarized in Table 1.

6. Conclusions

We presented in this paper updated estimates for the TRAPPIST-1 star. We proposed a new measurement of its parallax, 82.4 ± 0.8 mas, based on 188 epochs and 45,000 images with the TRAPPIST and Liverpool telescopes. This led to a revised luminosity of $L_* = (5.22 \pm 0.19) \times 10^{-4}\,L_\odot$, almost two times more precise than the previous estimate. We also proposed an updated mass based on two independent approaches, stellar evolution modeling and an empirical model-independent methodology based on astrometric binaries. We combined this

information to obtain the final stellar mass for TRAPPIST-1: $M_* = 0.089 \pm 0.006\,M_\odot$. Combined with stellar density from transits, this mass led to $R_* = 0.121 \pm 0.003\,R_\odot$, which, combined to luminosity, gave $T_{\rm eff} = 2516 \pm 41$ K.

The stellar parameters we propose in this paper represents a significant improvement compared to the priors used in previous transit analyses (Gillon et al. 2016, 2017), which were based on stellar evolution models only and correspond to a young star, which is discarded for TRAPPIST-1. The exact impact on planets' properties, particularly on their masses inferred from TTVs (hence on planetary densities), on their irradiation (hence on surface conditions and habitability), and on their atmospheric evolution (the contraction time onto the main sequence is $\sim$1.9 Gyr for a $0.09\,M_\odot$, compared to $\sim$5.8 Gyr for a $0.08\,M_\odot$) will be assessed in future studies (e.g., Delrez et al. 2018; Grimm et al. submitted).

We thank Trent Dupuy for discussions of VLMS binary masses. We are indebted to Gilles Fontaine and Pierre Brassard for having provided us EOS tables. We warmly thank the stellar physics team in Liege for their advices when developing ultracool stellar models. V.V.G. and M.G. are FRS-FNRS Research Associates. E.J. is an FRS-FNRS Senior Research Associate. C.S.F. is funded by an Action de Recherche Concertée (ARC) grant financed by the Wallonia–Brussels Federation. TRAPPIST-South is a project funded by the Belgian Fonds (National) de la Recherche Scientifique (FRS-FNRS) under grant FRFC 2.5.594.09.F, with the participation of the Swiss National Science Foundation (FNS/SNSF). TRAPPIST-North is a project funded by the University of Liège, and performed in collaboration with Cadi Ayyad University of Marrakesh. The research leading to these results has received funding from the European Research Council under the FP/2007-2013 ERC grant agreement No. 336480, and from the ARC grant for Concerted Research Actions, financed by the Wallonia–Brussels Federation. Our paper also uses data obtained at the Liverpool Telescope, which is operated on the island of La Palma by Liverpool John Moores University in the Spanish Observatorio del Roque de los Muchachos of the Instituto de Astrofisica de Canarias with financial support from the UK Science and Technology Facilities Council. This work was partially supported by a grant from the Simons Foundation (PI: Queloz, grant No. 327127). L.D. acknowledges support from the Gruber Foundation Fellowship. A.J.B. acknowledges support from the US-UK Fulbright Commission. B.-O.D. acknowledges support from the Swiss National Science Foundation (PP00P2-163967).

Software: CLES (Scuflaire et al. 2008).

ORCID iDs

Michael Gillon https://orcid.org/0000-0003-1462-7739
Adam J. Burgasser https://orcid.org/0000-0002-6523-9536
Brice-Olivier Demory https://orcid.org/0000-0002-9355-5165
Julien de Wit https://orcid.org/0000-0003-2415-2191
Didier Queloz https://orcid.org/0000-0002-3012-0316
Amaury H. M. J. Triaud https://orcid.org/0000-0002-5510-8751

References

Agol, E., Steffen, J., Sari, R., & Clarkson, W. 2005, MNRAS, 359, 567
Allard, F., Homeier, D., & Freytag, B. 2012a, RSPTA, 370, 2765
Allard, F., Homeier, D., Freytag, B., & Sharp, C. M. 2012b, in EAS Publications Ser. 57, Low-mass Stars and the Transition Stars/Brown Dwarfs (EES2011), ed. C. Reylé, C. Charbonnel, & M. Schultheis, 3
Asplund, M., Grevesse, N., Sauval, A. J., & Scott, P. 2009, ARA&A, 47, 481
Badnell, N. R., Bautista, M. A., Butler, K., et al. 2005, MNRAS, 360, 458
Baraffe, I., Homeier, D., Allard, F., & Chabrier, G. 2015, A&A, 577, A42
Barstow, J. K., & Irwin, P. G. J. 2016, MNRAS, 461, L92
Bochanski, J. J., Hawley, S. L., Covey, K. R., et al. 2010, AJ, 139, 2679
Boss, A. P., Weinberger, A. J., Keiser, S. A., et al. 2017, AJ, 154, 103
Bourrier, V., Ehrenreich, D., Wheatley, P. J., et al. 2017, A&A, 599, L3
Burgasser, A. J., Logsdon, S. E., Gagné, J., et al. 2015, ApJS, 220, 18
Burgasser, A. J., & Mamajek, E. E. 2017, ApJ, 845, 110
Burrows, A., Hubbard, W. B., Lunine, J. I., & Liebert, J. 2001, RvMP, 73, 719
Burrows, A., Marley, M., Hubbard, W. B., et al. 1997, ApJ, 491, 856
Caffau, E., Ludwig, H.-G., Steffen, M., Freytag, B., & Bonifacio, P. 2011, SoPh, 268, 255
Cassisi, S., Potekhin, A. Y., Pietrinferni, A., Catelan, M., & Salaris, M. 2007, ApJ, 661, 1094
Chabrier, G., & Baraffe, I. 1997, A&A, 327, 1039
Chabrier, G., Baraffe, I., Allard, F., & Hauschildt, P. 2000, ApJ, 542, 464
Chabrier, G., Gallardo, J., & Baraffe, I. 2007, A&A, 472, L17
Costa, E., Méndez, R. A., Jao, W.-C., et al. 2006, AJ, 132, 1234
de Wit, J., Wakeford, H. R., Gillon, M., et al. 2016, Natur, 537, 69
Delrez, L., Gillon, M., & Triaud, A. H. M. J. 2018, MNRAS, in press (arXiv:1801.02554)
Dupuy, T. J., & Liu, M. C. 2017, ApJS, 231, 15
Feiden, G. A., & Chaboyer, B. 2014a, ApJ, 789, 53
Feiden, G. A., & Chaboyer, B. 2014b, A&A, 571, A70
Ferguson, J. W., Alexander, D. R., Allard, F., et al. 2005, ApJ, 623, 585
Filippazzo, J. C., Rice, E. L., Faherty, J., et al. 2015, ApJ, 810, 158
Fontaine, G., Graboske, H. C., Jr., & van Horn, H. M. 1977, ApJS, 35, 293
Gillon, M., Jehin, E., Lederer, S. M., et al. 2016, Natur, 533, 221
Gillon, M., Jehin, E., Magain, P., et al. 2011, EPJWC, 11, 06002
Gillon, M., Triaud, A. H. M. J., Demory, B.-O., et al. 2017, Natur, 542, 456
Gizis, J. E., Monet, D. G., Reid, I. N., et al. 2000, AJ, 120, 1085
Grevesse, N., & Noels, A. 1993, in Origin and Evolution of the Elements, ed. N. Prantzos, E. Vangioni-Flam, & M. Casse (Cambridge: Cambridge Univ. Press), 15
Iglesias, C. A., & Rogers, F. J. 1996, ApJ, 464, 943
Jehin, E., Gillon, M., Queloz, D., et al. 2011, Msngr, 145, 2
Kervella, P., Mérand, A., Ledoux, C., Demory, B.-O., & Le Bouquin, J.-B. 2016, A&A, 593, A127
Luger, R., & Barnes, R. 2015, AsBio, 15, 119
Luger, R., Sestovic, M., Kruse, E., et al. 2017, NatAs, 1, 0129
MacDonald, J., & Mullan, D. J. 2014, ApJ, 787, 70
Magic, Z., Weiss, A., & Asplund, M. 2015, A&A, 573, A89
Mann, A. W., Deacon, N. R., Gaidos, E., et al. 2014, AJ, 147, 160
Metcalfe, T. S., Creevey, O. L., Doğan, G., et al. 2014, ApJS, 214, 27
Miglio, A., & Montalbán, J. 2005, A&A, 441, 615
Mullan, D. J., & MacDonald, J. 2001, ApJ, 559, 353
Porto de Mello, G. F., Lyra, W., & Keller, G. R. 2008, A&A, 488, 653
Potekhin, A. Y., Baiko, D. A., Haensel, P., & Yakovlev, D. G. 1999, A&A, 346, 345
Press, W. H., Teukolsky, S. A., Vetterling, W. T., & Flannery, B. P. 1992, Numerical Recipes in FORTRAN. The Art of Scientific Computing (Cambridge: Cambridge Univ. Press)
Rajpurohit, A. S., Reylé, C., Allard, F., et al. 2013, A&A, 556, A15
Reid, I. N., & Hawley, S. L. 2005, New Light on Dark Stars: Red dwarfs, Low-mass Stars, Brown Dwarfs (Chichester: Praxis)
Reiners, A., & Basri, G. 2010, ApJ, 710, 924
Saumon, D., Chabrier, G., & van Horn, H. M. 1995, ApJS, 99, 713
Scuflaire, R., Théado, S., Montalbán, J., et al. 2008, Ap&SS, 316, 83
Seager, S., & Deming, D. 2010, ARA&A, 48, 631
Spada, F., Demarque, P., Kim, Y.-C., & Sills, A. 2013, ApJ, 776, 87
Steele, I. A., Smith, R. J., Rees, P. C., et al. 2004, Proc. SPIE, 5489, 679
Torres, G. 2013, AN, 334, 4
Van Grootel, V., Charpinet, S., Brassard, P., Fontaine, G., & Green, E. M. 2013, A&A, 553, A97
Veyette, M. J., Muirhead, P. S., Mann, A. W., & Allard, F. 2016, ApJ, 828, 95
von Boetticher, A., Triaud, A. H. M. J., Queloz, D., et al. 2017, A&A, 604, L6
Weinberger, A. J., Boss, A. P., Keiser, S. A., et al. 2016, AJ, 152, 24
Winn, J. N. 2010, in Exoplanet Transits and Occultations, ed. S. Seager (Tucson, AZ: Univ. Arizona Press), 55
Xu, Y., Takahashi, K., Goriely, S., et al. 2013, NuPhA, 918, 61